

Ordering Kinetics in Quasi-One-Dimensional Ising-Like Systems

M. Müller¹ and W. Paul¹

Received April 6, 1993; final June 3, 1993

We present results of a Monte Carlo simulation of the kinetics of ordering in the two-dimensional nearest-neighbor Ising model in an $L \times M$ geometry with two free boundaries of length $M \gg L$. This model can be viewed as representing an adsorbant on a stepped surface with mean terrace width L . We follow the ordering kinetics after quenches to temperatures $0.25 \leq T/T_c \leq 1$ starting from a random initial configuration at a coverage of $\theta = 0.5$ in the corresponding lattice gas picture. The systems evolve in time according to a Glauber kinetics with nonconserved order parameter. The equilibrium structure is given by a one-dimensional sequence of ordered domains. The ordering process evolves from a short initial two-dimensional ordering process through a crossover region to a quasi-one-dimensional behavior. The whole process is diffusive (inverse half-width of the structure factor peak $1/\Delta q_{\parallel} \propto \sqrt{t}$), in contrast to a model proposed by Kawasaki *et al.*, where an intermediate logarithmic growth law is expected. All results are completely describable in the picture of an annihilating random walk (ARW) of domain walls.

KEY WORDS: Adsorption on stepped surfaces; annihilating random walk; kinetic Ising model; Monte Carlo simulation; quasi-one-dimensional ordering kinetics; stochastic processes.

1. INTRODUCTION

The ordering kinetics at surfaces has been of long-standing theoretical interest (for reviews see refs. 1–6) and has also been the aim of experimental investigations.^(7–12) The understanding of these processes is also of great technological importance in material science for questions concerning catalysis and corrosion, for instance. While on an ideal two-dimensional substrate of infinite extension the cluster size grows as \sqrt{t} , where t

¹ Institut für Physik, Johannes Gutenberg Universität, W-6500 Mainz, Germany. E-mail: mueller@meichior.physik.uni-mainz.de

measures the time after the adatom adsorption into an initially completely random configuration, deviations from this behavior are expected for non-ideal surfaces showing defects, for example, surface steps. In previous work it has been shown that even a simple model for perfectly regular surface steps shows a rich variety of ordering phenomena already in thermal equilibrium.^(13–16) The kinetics of this ordering process can be expected to show the usual signature of two-dimensional coarsening at the beginning and then a crossover to a quasi-one-dimensional behavior. For ordering processes which can be treated as being quasi-one-dimensional (as a result of geometry as here or because of highly anisotropic interactions) Kawasaki and co-workers have developed a theory describing the ordering domains as an ensemble of interacting kinks and antikinks.^(17–20) In this model the walls move under the influence of an exponentially decaying deterministic force between the walls and an additional stochastic force. They argued that for an intermediate time one could neglect the influence of the stochastic force, which would then lead to a logarithmic growth law of the mean domain size. We will show that this theory does not apply to our model, but that instead a description with a purely stochastic wall movement in the framework of annihilating random walk (ARW)^(21–29) is in complete and detailed agreement with the ordering kinetics our model exhibits. In Section 2 we explain the model and the simulation technique; in Section 3 we discuss a mean field approximation of the ordering kinetics and the qualitative predictions one can derive from it. Several alternative measures for the mean domain size and their interrelations are discussed in Section 4 and applied to the analysis of the growth behavior of the domains in the two-dimensional regime in Section 5 and to that of the one-dimensional regime in Section 6. Section 7 finally gives our conclusions.

2. MODEL AND SIMULATION TECHNIQUE

We study a two-dimensional nearest-neighbor Ising model which can be defined with the lattice gas Hamiltonian with the occupation numbers c_i

$$\beta H = \Phi \sum_{\langle ij \rangle} c_i c_j + \varepsilon \sum_{\text{bulk}} c_i + \varepsilon_e \sum_{\text{edge}} c_i \quad (1)$$

The corresponding magnetic Hamiltonian [$c_i = (1 + s_i)/2$] is given by

$$\beta H = -J \sum_{\langle ij \rangle} s_i s_j + h \sum_{\text{bulk}} s_i + h_e \sum_{\text{edge}} s_i \quad (2)$$

with

$$J = -\frac{\Phi}{4} \quad (3)$$

$$h = \Phi + \frac{\varepsilon}{2} \quad (4)$$

$$h_e = \frac{3}{4}\Phi + \frac{\varepsilon_e}{2} \quad (5)$$

where we confine ourselves to the case $J > 0$ and $h = h_e = 0$.⁽¹⁶⁾ In the thermodynamic limit $L, M \rightarrow \infty$ the system is the usual two-dimensional Ising model with a critical coupling $J_c = (\ln 1 + \sqrt{2})/2$. For fixed terrace width L and $M \rightarrow \infty$ the system is quasi one-dimensional and for small enough temperatures breaks up into a sequence of domains of size^(30,31) $\xi_{||} = \sqrt{L} \exp(f_{\text{int}} L/k_B T)$, where f_{int} is the excess free energy of a domain wall. The static finite-size and critical properties of this model have been investigated in detail in a series of papers.⁽¹³⁻¹⁶⁾ We follow the approach to this equilibrium configuration starting from a homogeneous $T = \infty$ configuration,

$$P(s_1, s_2, \dots, s_{LM}, 0) = \frac{1}{LM} \quad (6)$$

The kinetics applied is the single-spin-flip Glauber kinetics using Metropolis rates,

$$\begin{aligned} \partial_t P(s_1, \dots, s_j, \dots, s_{LM}, t) = & \sum_{j=1}^{LM} W(-s_j \rightarrow s_j) P(s_1, \dots, -s_j, \dots, s_{LM}, t) \\ & - \sum_{j=1}^{LM} W(s_j \rightarrow -s_j) P(s_1, \dots, s_j, \dots, s_{LM}, t) \quad (7) \end{aligned}$$

$$W(-s_j \rightarrow s_j) = \frac{1}{\tau} \min(1, \exp(-\beta \Delta H(s_1, \dots, s_{LM})))$$

All observables are averages over typically 1000 realizations of the Markov chain defined by Eq. (7).

3. MEAN FIELD APPROXIMATION FOR THE KINETICS

Let us now first try to get a qualitative understanding of the quasi-one-dimensional phase of the ordering process by looking at a mean field approximation of the kinetic equation (7). The ordering process in this

stage will be determined by the kinetics of domain walls. We will substitute the value of the spin variable $s(i, j)$ by

$$s(i, j) \rightarrow m_i = \frac{1}{L} \sum_{j=0}^{L-1} s(i, j) \quad (8)$$

and approximate the energy change ΔH as being only dependent on m_i . This changes (7) to a master equation for the row magnetizations m_i and by performing a Kramers–Moyal expansion in the inverse width of the strip (proportional to change of m_i due to a single spin flip), one arrives at a Fokker–Planck equation,

$$\partial_t P(\{m\}, t) = \sum_{k=1}^M \partial_{m_k} (U'_k P) + \frac{1}{2} \sum_{k=1}^M \partial_{m_k}^2 (D_k P) \quad (9)$$

where

$$U'_k = (1 + m_k) \min \left(1, \exp \left\{ -2J \left[\left(4 - \frac{2}{L} \right) m_k + \partial_{\parallel}^2 m_k \right] \right\} \right) \\ - (1 - m_k) \min \left(1, \exp \left\{ 2J \left[\left(4 - \frac{2}{L} \right) m_k + \partial_{\parallel}^2 m_k \right] \right\} \right) \quad (10)$$

$$D_k = \frac{2}{L} (1 + m_k) \min \left(1, \exp \left\{ -2J \left[\left(4 - \frac{2}{J} \right) m_k + \partial_{\parallel}^2 m_k \right] \right\} \right) \\ + \frac{2}{L} (1 - m_k) \min \left(1, \exp \left\{ 2J \left[\left(4 - \frac{2}{J} \right) m_k + \partial_{\parallel}^2 m_k \right] \right\} \right) \quad (11)$$

This equation is highly nonlinear in the row magnetization and its variations along the strip. Each row magnetization changes according to a local potential $U_k(m_{k-1}, m_k, m_{k+1})$ depending on the magnetization of the neighboring rows and under the influence of a diffusion coefficient $D_k(m_{k-1}, m_k, m_{k+1})$ of similar form. In the case of a homogeneous magnetization $m_k = m, \forall k$, the mean field critical temperature of the finite strip can be read off as the temperature where the kinetic potential $U(m)$ develops a double-well structure,

$$T_C^{\text{MF}}(\infty) - T_C^{\text{MF}}(L) = \frac{2}{L} \quad (12)$$

in qualitative accordance with the MC simulations.⁽¹³⁾ A qualitative analysis of the potentials U_k allows us to identify the kinetics that will result from such a Fokker–Planck equation. First of all, since the row

magnetization has to change from m_{sp} to $-m_{sp}$ in a finite number of steps, the potentials allow for a stable multikink solution of the Fokker-Planck equation. When one looks at a row magnetization m_k whose neighbors are $m_{k-1} = m_{sp}$ and $m_{k+1} = -m_{sp}$ (at low temperatures the width of the domain walls will approach one lattice spacing) the corresponding potential shows the stable values $\pm m_{sp}$ separated by a barrier (see left side of Fig. 1). Such an isolated domain wall will therefore undergo an activated diffusion process. On the other hand, a row with $m_k = -m_{sp}$ and neighbors $m_{k-1} = m_{sp} = m_{k+1}$ experiences a strong drift toward m_{sp} (right side of Fig. 1). Therefore adjacent domain walls attract each other across a distance equal to the width of the walls and annihilate on contact.

It is also quite instructive to look at the Langevin equation corresponding to the thus derived Fokker-Planck equation close to T_C where one can expand the potentials and the diffusion coefficients in powers of $T - T_C$ and where we will furthermore perform a continuum limit,

$$\partial_t m(x, t) = \Gamma \left(m - \frac{M^3}{M_0^2} + \frac{1}{2} \xi^2 \partial_x^2 m \right) + (D[m])^{1/2} \zeta(x, t) \quad (13)$$

with the kinetic coefficient

$$\Gamma = 8 \left(1 - \frac{2}{L} \right) (J - J_C) \quad (14)$$

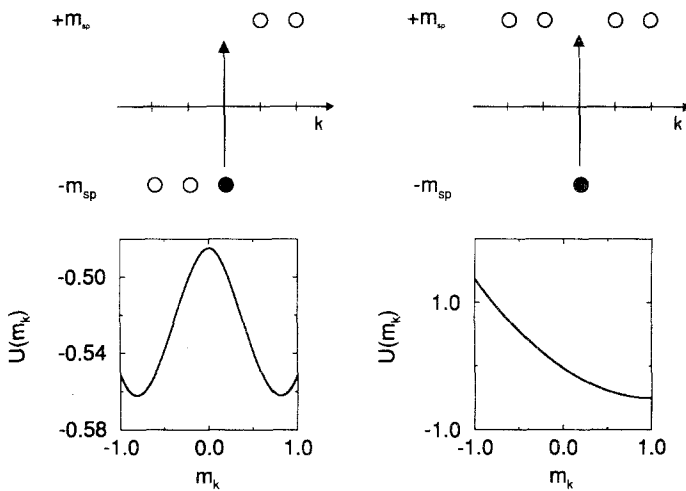


Fig. 1. Kink configurations and the corresponding mean field drift potential for magnetization m_k . (Left) Isolated wall at position k ; (right) two walls meeting at position k and annihilating on contact.

the equilibrium magnetization

$$M_0^2 = \frac{J - J_c}{4(1 - 2/L) J^2 [1 - (8/3)(1 - 2/L)J]} \quad (15)$$

the diffusion coefficient

$$D[m] = \frac{4}{L} \left\{ 1 - 4 \left(1 - \frac{2}{L} \right) J m + 64 \left(1 - \frac{2}{L} \right)^2 J^2 \right. \\ \left. \times \left[1 - \frac{3}{8} \left(1 - \frac{2}{L} \right) J \right] m^3 - 4J \partial_x^2 m \right\} \quad (16)$$

and a Gaussian white noise

$$\langle \zeta(x, t) \rangle = 0, \quad \langle \zeta(x, t) \zeta(x', t') \rangle = \delta(x - x') \delta(t - t') \quad (17)$$

This equation only has stationary one-kink solutions of the form

$$m^{\text{kink}} = M_0 \tanh \frac{x}{\xi} \quad (18)$$

and is the starting point for Kawasaki's^(17,18) derivation of a kinetic equation for the position of the kinks showing an exponentially decaying interaction between adjacent domain walls. This interaction gives rise to an intermediate growth law for the domain sizes

$$\langle l(t) \rangle \propto \ln t \quad (19)$$

if one neglects the stochastic forces. One should note, however, that this long-range interaction between the domain walls is created in the above analysis of our system by performing the continuum limit. The discrete row magnetizations reach their equilibrium values across a domain wall in a finite number of steps, leading to an interaction between adjacent kinks of strictly finite range. Consequently, the discrete equations have stationary multikink solutions, in contrast to the continuum treatment. The ordering process would just freeze without the stochastic forces. This discrepancy is one of the reasons Kawasaki's treatment is not applicable to the ordering kinetics in our system, as we will show in the following sections. This will hold true also in other cases where the discreteness of states cannot be left out of the description. The other reason is connected with this one. Since the coupling constants of the spins is the same parallel and perpendicular to the strip, the minimal domain size $l(t_{\text{cross}})$ in the regime of one-dimensional ordering $l(t_{\text{cross}}) \propto L$ is much larger than the interaction range

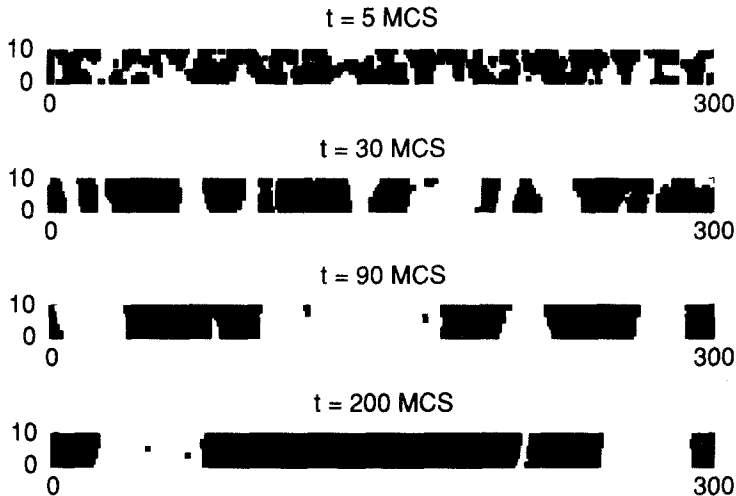


Fig. 2. Four snapshots at the indicated times of a sample realization of the stochastic domain growth kinetics. Plus spins in black. There are periodic boundary conditions in the long direction.

$\xi \propto \sqrt{L}$. In the case of strictly finite interaction range there can be no time scale on which the influence of the stochastic force on the movement of the kinks is negligible.²

To summarize, the mean field treatment shows that we will have to expect a kinetics describable by domain wall diffusion of isolated walls and a fast annihilation process of walls approaching each other to within a distance equal to the width of the walls.

4. MEASURING THE DOMAIN SIZE

In Fig. 2 we show snapshots of a typical stochastic realization of the ordering process in the early two-dimensional stage $t=5$ MCS and the later quasi-one-dimensional stage $t=30$ MCS, $t=90$ MCS, and $t=200$ MCS. A domain wall in this picture would be the boundary of a cluster of, say, plus spins which reaches from one side of the strip to the other. The position of this domain wall is defined as its average position along the strip. We furthermore have to distinguish between the bulk of a domain wall and the domain wall. One can get an estimate for the thickness of the domain walls by treating them in an SOS approximation.

²This qualitative behavior is also expected for quasi-one-dimensional ordering in three-dimensional systems if the interaction is isotropic.

The result is $\xi = (2L)^{1/2} \exp(-J)$ and shows the random walk character of the wall. Using this result, we define the bulk of a domain to be the region $x_i + \xi \leq x \leq x_{i+1} - \xi$, where x_i and x_{i+1} are the positions of the bounding domain walls. Now we can define the mean squared magnetization inside the domains by

$$\langle m_T^2 \rangle = \left\langle \left(\frac{\sum_i |m_i| l_i}{\sum_i l_i} \right)^2 \right\rangle \quad (20)$$

where the magnetization inside one domain is given as

$$m_i = \frac{\sum_{j \text{ in domain } i} S_j}{L(l_i - 2\xi)} \quad (21)$$

During the two-dimensional early stages of the ordering process this mean squared magnetization thermalizes and reaches the equilibrium value around the crossover time to the quasi-one-dimensional behavior.

The above geometrical considerations allow for two ways of defining the mean domain size. If we take the angular brackets $\langle \dots \rangle$ to denote an average over the stochastic realizations of the ordering process and the square brackets with an index k $[\dots]_k$ to denote an average taken in the k th realization we can define the mean domain size as

$$l_1(t) = \langle [l]_k \rangle = \sum_{l=1}^M l P(l, t) \quad (22)$$

where $P(l, t) = \langle P_k(l, t) \rangle$ is the average domain size distribution. An alternative definition uses the mean number of domain walls

$$l_2(t) = \frac{M}{N(t)} \quad (23)$$

Since $[l]_k = M/N_k$ one easily derives

$$\frac{l_1}{l_2} - 1 = \sum_{i=2}^{\infty} (-1)^i \left\langle \left(\frac{[l]_k - \langle [l]_k \rangle}{\langle [l]_k \rangle} \right)^i \right\rangle \approx \frac{\langle N_k^2 \rangle - \langle N_k \rangle^2}{\langle N_k \rangle^2} \geq 0 \quad (24)$$

Both definitions give rise to self-averaging observables and lead to

$$\frac{\Delta l}{l} \propto \frac{1}{(MN_{\text{iter}})^{1/2}} \quad (25)$$

where N_{iter} is the number of realizations of the Markov chain. This behavior could be nicely seen in our simulations. Furthermore, the exact

asymptotic behavior in $1/M$ can be calculated by resorting to the annihilating random walk as an asymptotically equivalent model, but this will be discussed in more detail in a separate publication.⁽³⁶⁾

Let us now make contact with experimentally accessible methods to measure the domain size. One such quantity is the incoherent dynamic structure factor measured, for instance, in LEED or neutron scattering experiments,

$$S(\mathbf{q}, t) = \frac{1}{L^2 M^2} \left\langle \left| \sum_{\mathbf{x}} s(\mathbf{x}, t) \exp(i\mathbf{q} \cdot \mathbf{x}) \right|^2 \right\rangle \quad (26)$$

Most notably, its value at the peak at $\mathbf{q} = 0$ is given by the mean squared magnetization in the whole system,

$$\langle m^2 \rangle(t) = \left\langle \left(\sum_{\mathbf{x}} s(\mathbf{x}, t) \right)^2 \right\rangle = S(0, t) \quad (27)$$

The peak height itself is only an approximate measure for the domain size and we now want to relate it to the more microscopic definitions given above. Suppose we are looking at the later stages of the ordering process in the k th realization of the Markov chain. There are N_k domains of length l_i and magnetization m_i^k which we furthermore assume to be thermalized, $m_i^k = \pm m_T$. The overall magnetization in the k th realization is then given as

$$m_k = \frac{m_T}{M} \sum_{i=0}^{N_k-1} (-1)^i l_i \quad (28)$$

and the mean squared magnetization as

$$\begin{aligned} m_k^2 &= \frac{m_T^2}{M^2} \sum_{i,j=0}^{N_k-1} (-1)^{i+j} l_i l_j \\ &= \frac{m_T^2}{M^2} N_k \sum_{r=0}^{N_k-1} (-1)^r ([l_i l_{i+r}]_k - [l]_k^2) \end{aligned} \quad (29)$$

Here we use a periodic numbering of the domains and the domain length correlation function is independent of i after averaging with the distribution for the k th realization. In a separate paper⁽³⁶⁾ we will discuss these correlations in more detail with respect to the ARW, but let us here suppose that the correlations vanish for $r \neq 0$, which after averaging over the stochastic

realizations leads to a relation between the mean squared magnetization and the domain size as measured by l_2 :

$$\langle m^2 \rangle = \frac{m_T^2}{M} \alpha l_2 \quad (30)$$

$$\alpha = \frac{1}{l_2} \left\langle \frac{[l^2]_k - [l]_k^2}{[l]_k} \right\rangle$$

Figure 3 is a test of this relation for a low temperature $T=0.5T_C$ and several values for the width of the system. After a stronger initial time dependence the ratio of the two sides of Eq. (30) is more or less constant and equal to 1 to within 10%. The discrepancy almost is within the experimental uncertainty for the determination of the mean squared magnetization (5%) and the mean squared magnetization inside a domain (2%). This means that for the system size under study, $M=1000$, the correlations between adjacent domain sizes are not very important.

Finally, there is the inverse of the half-width of the structure factor peak $1/\Delta q_{||}$, which is a measure for the size of correlated spin clusters during all of the ordering process. For short times where the kinetics is two dimensional and does not feel the width of the strip both half-widths $\Delta q_{||}$ and Δq_{\perp} are identical and measure the size of two-dimensional growing clusters and in the quasi-one-dimensional regime $\Delta q_{||}$ measures the size of

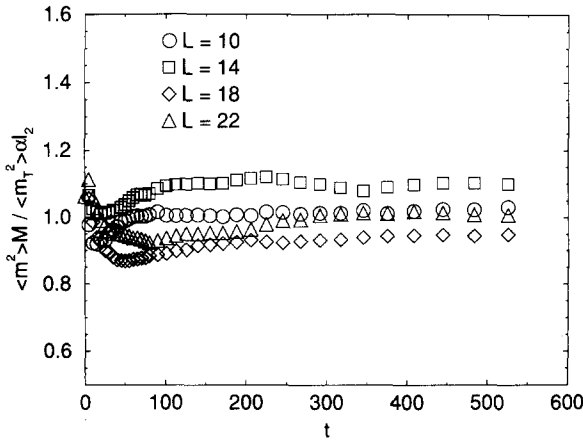


Fig. 3. Test of the relation between the mean squared magnetization in the system $\langle m^2 \rangle$, the mean magnetization inside a domain $\langle m_T^2 \rangle$, and the mean domain size as measured by the mean number of domain walls l_2 . Different symbols stand for different widths of the strip as given in the figure.

the domains. During the whole ordering process we can get the dynamic structure factor from a 2-dimensional Fourier transform of the spin pair correlation function properly taking into account the periodic boundary conditions along the strip and the finite extension perpendicular to it. But in the late stages it is easier to obtain the dynamic structure factor from the domain size distribution. So let us assume a one-dimensional structure of row magnetizations m_j . Following a derivation given by Kawasaki,⁽¹⁷⁾ the dynamic structure factor is then given by

$$\begin{aligned} S(q) &= \left\langle \frac{1}{M^2} \left| \sum_j m_j \exp(iqj) \right|^2 \right\rangle \\ &= \frac{1}{M^2} \sum_{jk} \langle m_j m_k \rangle \exp[iq(j-k)] \\ &= \frac{1}{4M^2 \sin^2(q/2)} \sum_{jk} \langle (m_{j+1} - m_j)(m_{k+1} - m_k) \rangle \exp[iq(j-k)] \end{aligned}$$

where the last equality holds due to the periodic boundary conditions. Let us now furthermore assume that the domain magnetizations have reached their equilibrium value and that we have sharp domain walls,

$$m_{k+1} - m_k = 2m_T \sum_r (-1)^r \delta_{k,x_r} \quad (31)$$

where x_r is the position of the r th domain wall. Assuming furthermore that adjacent domain sizes are uncorrelated and that the number of domains in the system is large, one derives

$$\begin{aligned} S(q) &= \frac{m_T^2}{M^2 \sin^2(q/2)} \sum_{jk} \sum_{r,s} \langle (-1)^{r+s} \delta_{j,x_r} \delta_{k,x_s} \rangle \exp[iq(j-k)] \\ &= \frac{m_T^2}{M^2 \sin^2(q/2)} \left\langle N_k \left(1 + \Re 2 \sum_{\Delta r > 0} (-1)^{\Delta r} [\exp(iql)]_k^{\Delta r} \right) \right\rangle \\ &= \frac{m_T^2}{M} \left\langle l_k \frac{1 - |\exp(iql)|_k^2}{l_k^2 \sin^2(q/2) |1 + [\exp(iql)]_k|^2} \right\rangle \quad (32) \end{aligned}$$

For q not too small one can furthermore use the self-averaging properties of the domain size distribution to substitute the averages in a single realization of the Markov chain, $[\dots]_k$, by an average with the mean domain size distribution, $\langle \dots \rangle$.

$$S(q) = \frac{m_T^2}{M} \frac{1 - |\langle \exp(iql) \rangle|^2}{l \sin^2(q/2) |1 + \langle \exp(iql) \rangle|^2} \quad (33)$$

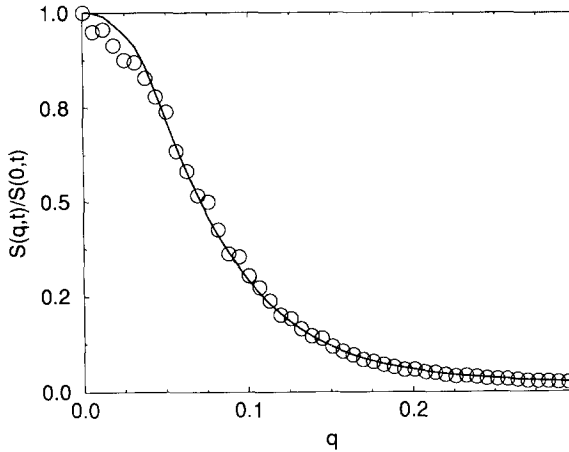


Fig. 4. Comparison of the dynamic structure factor as measured by a Fourier transform of the spin pair correlation function (open circles) and by a Fourier transform of the domain size distribution (full curve). The time chosen belongs to the regime of the one-dimensional ordering.

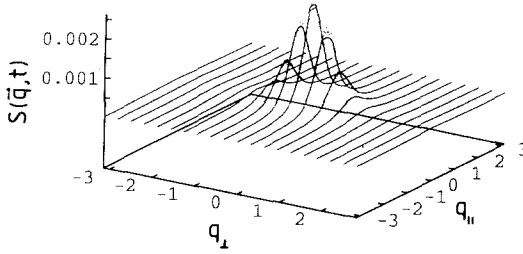
If the mean domain size l is much larger than the domain wall thickness, we can approximate $\sin^2(q/2) \approx q^2/4$ and recover the result by Kawaski.⁽¹⁷⁾ Figure 4 presents a comparison of the dynamic structure factor obtained from the spin pair correlation function to that obtained from the mean domain size distribution. The parameters are chosen such as to make the approximations made in the derivation justifiable and we see that the two curves show only a small difference at the smallest q values.

In the next two sections we will analyze the ordering process in terms of the different length measures discussed here and their interrelations.

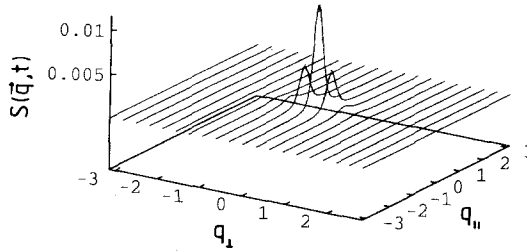
5. THE REGIME OF TWO-DIMENSIONAL GROWTH

The growth of the small two-dimensional clusters in the beginning is curvature driven and leads to a diffusive growth of the mean size of the two-dimensional clusters $l'(t) \propto \sqrt{t}$.^(33,34) This behavior will cross over to quasi-one-dimensional growth when the mean cluster size is equal to the width of the strip $t_{\text{cross}} \propto L^2$. The two-dimensional growth and crossover to one-dimensional behaviour are nicely seen in Fig. 5, where we show the dynamic structure factor for three different times. At short times it shows a symmetric peak the width of which decreases with time. At intermediate times the peak gets asymmetric and finally there is no structure left in the direction perpendicular to the strip and only $S(q_{\parallel}, q_{\perp} = 0)$ contains

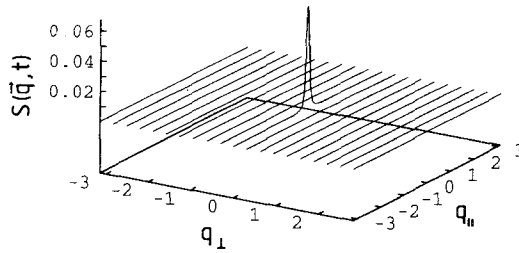
structural information. In this regime the mean squared magnetization is proportional to the area of the cluster $[\langle m^2 \rangle(t)]^{1/2} \propto l'(t)$, and one can get a nice scaling plot by plotting $S(q_{\parallel} l', q_{\perp} = 0) / \langle m^2 \rangle(t)$ against $q_{\parallel} l'(t)$. This is all just standard two-dimensional behavior. During this same period the mean squared magnetization inside a domain approaches its equi-



(a)



(b)



(c)

Fig. 5. Dynamic structure factor for the early stages of the ordering process. (a) $t = 5$ MCS shows a two-dimensional coarsening at the beginning. (b) At $t = 25$ MCS the dynamic structure factor is asymmetric as the correlation length ξ_{\perp} approaches its limiting value L . (c) For $t = 587$ MCS there is only structure along the strip showing up at $q_{\perp} = 0$.

librium value. We know that we have to expect a crossover time proportional to L^2 , so let us assume the following crossover scaling

$$\langle m_T^2(t) \rangle = m_T^2 f\left(\frac{t}{L^2}\right) \quad (34)$$

where the scaling function f should have the following limits:

$$\begin{aligned} f(x) &\rightarrow cx & \text{for } x &\rightarrow 0 \\ f(x) &\rightarrow 1 & \text{for } x &\rightarrow \infty \end{aligned}$$

Figure 6 shows the expected scaling behavior for a set of temperatures and strip widths given in the figure caption. The three different sets of data are for the three different temperatures used in the plot. The function f of course contains a temperature-dependent rate constant. The data for the lowest temperature furthermore asymptotically approach the highest value for the equilibrium magnetization. The raw data for the temperature dependence of this quantity suggest a crossover time of around $1.5L^2$.

Let us now look at the time dependence of the length scales defined by $1/\Delta q_{||}$ and $\langle m^2 \rangle$ which are applicable both in the one-dimensional and in the two-dimensional regime. Figure 7 shows them plotted against \sqrt{t} . The inverse width of the structure factor, which is the direct measure of the size

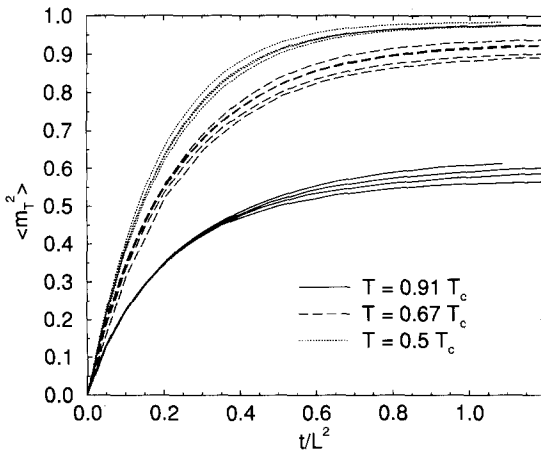


Fig. 6. Relaxation of the mean squared magnetization inside a domain plotted against the scaling variable t/L^2 . The full curves for $T=0.91T_c$ are for the system sizes $L=10, 14, 18, 22$, the long-dashed curves for $T=0.67T_c$ are for $L=7, 10, 13, 16, 25$, and those for $T=0.5T_c$ are for $L=10, 14, 18, 22$.

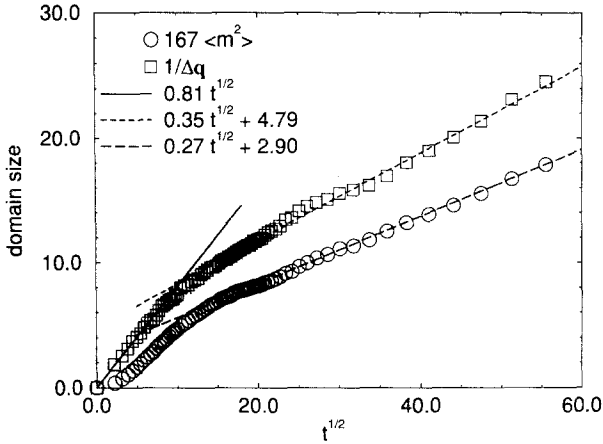


Fig. 7. Mean domain size as a function of time as measured by the mean squared magnetization in the system (open circles) and the inverse half-width of the structure factor peak (open squares). The curves are fits with a \sqrt{t} dependence. For the inverse half-width this holds in the two-dimensional and the one-dimensional regime. The mean squared magnetization in the two-dimensional regime would be proportional to t . There is no evidence for a logarithmic growth of the characteristic lengths at intermediate times.

of correlated spin clusters in both regimes, shows a nice linear dependence on \sqrt{t} . Only the slope changes between the two regimes, reflecting a changing rate constant. But also the mean squared magnetization is describable by a linear time dependence in the two-dimensional regime (parabolic shape at small t in the plot) crossing over to a dependence linear in \sqrt{t} in the quasi-one-dimensional regime. There is no convincing evidence for an intermediate logarithmic behavior. There is, however, a compatibility with a logarithmic behavior for times around the crossover time,⁽³²⁾ as shown in the inset of Fig. 8. This would correspond to the logarithmic growth law predicted in the picture of interacting kinks and antikinks in the work of Kawasaki and co-workers. If we, however, compare the domain size distribution at this time $t = 150$ MCS with the one predicted by the model of Kawasaki (full curve in Fig. 8), we find severe differences. The behavior for domains large compared to the mean domain size is described correctly, but this region is completely determined by having a Poissonian starting distribution (as is natural for domains created by a random two-dimensional coarsening along the strip) and a self-similar growth law. It is for the small domain sizes that the actual growth law matters. And here we definitely do not see a cutoff domain size and consequently our peak height is reduced with respect to the prediction of Kawasaki's model. The broken curve in Fig. 8 is a Monte Carlo simula-

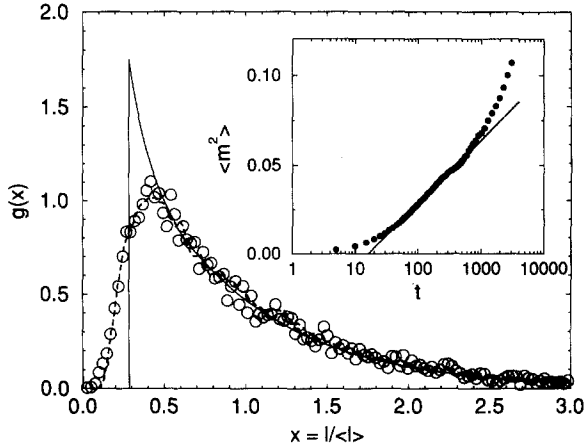


Fig. 8. Scaling plot of the domain size distribution function as measured in the Monte Carlo simulation of the Ising model (open circles) compared to the prediction of the theory of Kawasaki (full curve) and the simulation of an annihilating random walk of domain walls with a finite width which was adjusted to give the ideal matching (broken curve).

tion of a slightly modified ARW. We have included in the simulation the effect of a finite domain wall thickness ($\xi = 4$), which corresponds to the fact that in the Ising simulation two domain walls annihilate when their outermost points touch and not when their mass centers coincide. There is a perfect agreement between the ARW result and the result of the Ising simulation showing that the whole ordering process is diffusion controlled. There is no time regime where we could neglect the influence of the stochastic forces or detect an evidence of domain walls interacting with an exponentially decaying potential. As already discussed in Section 2, this might be due to an intrinsic difference between a model with discrete states and a theoretical description that uses a continuum approximation. We will find further prove that the ARW is the right description for the ordering process in our model when we now switch to the behavior in the one-dimensional regime.

6. THE REGIME OF ONE-DIMENSIONAL ORDERING

Figure 9 shows the time dependence of the mean domain size as measured by $l_1(t)$, i.e., the mean distance between the center positions of domain walls. There is a clear proportionality to \sqrt{t} starting in the crossover region between two-dimensional and one-dimensional growth behavior and holding as long as the overall magnetization in the system is not too close to its equilibrium value. There the self-similar growth law

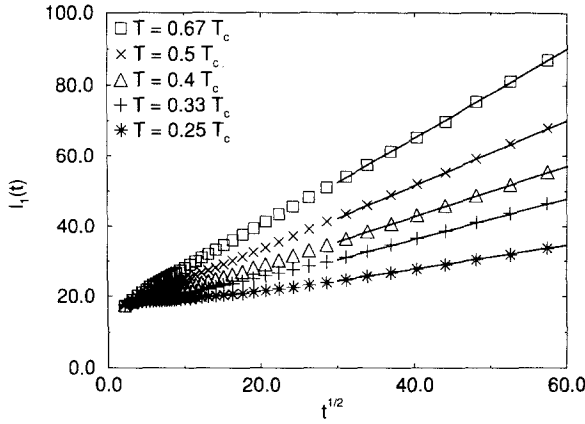


Fig. 9. Mean distance between adjacent domain walls for a set of temperatures indicated in the figure. The asymptotic straight lines are used to determine the diffusion coefficient of the domain walls.

would no longer hold and one gets an equilibrium domain size distribution maintained by domain wall annihilation and creation. The square root behavior for all times is also the prediction of the ARW, for which one derives

$$l(t) = (4\pi pt)^{1/2} \quad (35)$$

where $1/p$ is the rate of displacement of one domain wall. For low temperatures one can derive a prediction for this rate. The domain walls will then preferably run straight across the terrace. To move such a wall one needs a nucleating event where one spin in an adjacent row is flipped. This is most easily done for the spins at the edges of the terrace, where it creates only two broken bonds. Thus the probability for creating such a kink on a wall can be written as

$$p_{\text{nucl}} = \exp(-2J) \quad (36)$$

Flipping the neighborhood spin now costs no energy, so that this kink performs a symmetric random walk on the wall. Let p_L denote the probability to reach L , starting from 1. This is given by the probability of reaching $L-1$, p_{L-1} times the probability of not reaching zero, starting from $L-1$:

$$p_L = p_{L-1}(1 - p_L) = \frac{1}{1 + 1/p_{L-1}} = \frac{1}{L} \quad \text{since } p_1 = \frac{1}{L} \quad (37)$$

Since there are four spins on the edges of the wall, the mean rate of displacement of the wall can be written as

$$p = \frac{4}{L} \exp(-2J) \quad (38)$$

and we get a growth law for the mean domain size at low temperatures

$$l(t) = (dt)^{1/2} \quad \text{with diffusion constant} \quad d = \frac{16\pi}{L} \exp(-2J) \quad (39)$$

For temperatures approaching T_C the diffusion coefficient of the wall should exhibit an algebraic divergence

$$d \propto (J - J_C)^{-\gamma} \quad (40)$$

with $\gamma = 3/2$ in mean field theory. In Fig. 10 we show L times the diffusion coefficient of the wall measured by $l_1(t) : d_1$, respectively $l_2(t) : d_2$. The broken curve is the predicted Arrhenius-like behavior for low temperatures and nicely describes the data. The straight line for temperatures closer to T_C is a fit to an algebraic divergence with an exponent $\gamma = 0.69$. The error in the diffusion constants measured for these temperatures is rather large, however, because there is only a short time regime between the two-dimen-

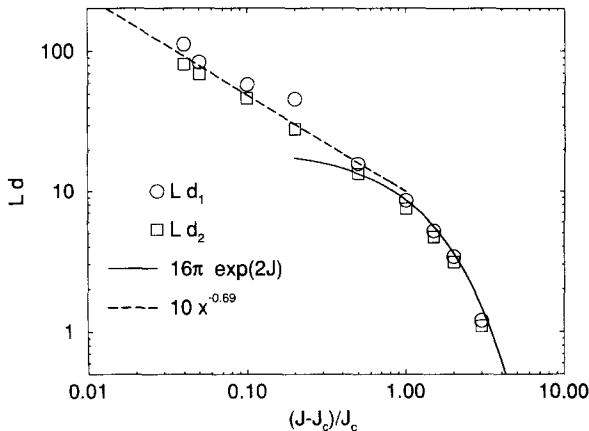


Fig. 10. Diffusion coefficient of a domain wall times the width of the strip as a function of the distance to the critical point. As the $1/L$ dependence of the diffusion coefficient is factored out explicitly, the plot contains data for different strip widths. Open circles are the diffusion coefficient from $l_1(t)$ measurements, open squares are from $l_2(t)$. The full curve is the predicted Arrhenius behavior at low temperatures. The dashed curve is the fit of an algebraic dependence for temperatures close to T_C .

sional growth and the asymptotic approach to equilibrium where the domain wall diffusion can be measured. Thus the exponent should be only taken as proving non-mean-field behavior and is no prediction for the Ising exponent that is to be expected approaching T_C .

We have already shown in Fig. 8 that the domain size distribution as seen in the Ising simulation can be perfectly described by an ARW with a finite domain wall thickness. Let us now have a look at the pair correlation function along the strip. The equivalence of the ARW to the kinetic Ising model at $T=0$ ⁽²⁶⁻²⁸⁾ gives a prediction for the pair correlation function of the Ising model along the strip when lengths are measured in units of the mean domain size,

$$G(x, t) = \operatorname{erfc}\left(\frac{\sqrt{\pi x}}{\langle l(t) \rangle}\right) \quad (41)$$

To test this equivalence we compare the simulation results in the Ising model for $M=1000$, $L=10$, $T=0.5T_C$, and $t=2000$ MCS with a mean domain size of $\langle l \rangle = 55.6$ with a simulation of an ARW with a wall thickness $\Delta=4$ at a number of walker steps where the mean domain size in the ARW simulation is $\langle l \rangle = 50.5$. Figure 11 shows the perfect agreement between the two models if lengths and times are scaled according to Eq. (41). To continue the information on the structural properties during the ordering process, let us now look at the dynamic structure factor in the quasi-one-dimensional time regime. Figure 12 shows a scaling plot of

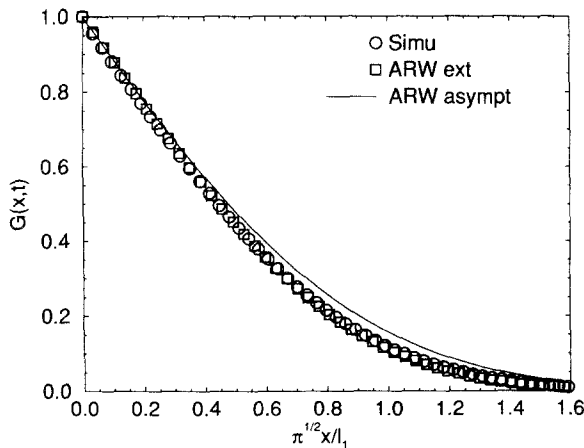


Fig. 11. Spin pair correlation function of the Ising system (circles) compared to the behavior of an ARW with finite domain wall thickness (squares). The full curve is the prediction for an ARW of point particles (ARW asympt).

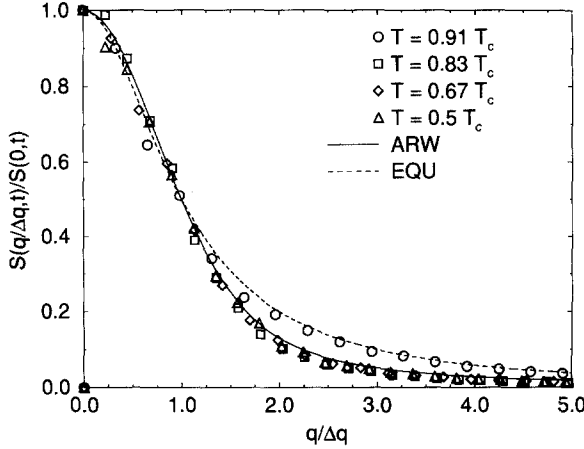


Fig. 12. Scaling plot for the dynamic structure factor in the one-dimensional growth regime. The three lower temperatures nicely follow the prediction for the ARW (full curve). For the time used in the plot the system with highest temperature is already close to equilibrium, as a comparison with the Ornstein-Zernicke prediction shows (broken curve), and is therefore not describable by the self-similar growth in the ARW.

the dynamic structure factor at $q_{\perp} = 0$, where we have taken $1/\Delta q_{\parallel}(t)$ as the relevant length scale measurement. The data at the lower temperatures show a nice scaling behavior in perfect accord with the analytic prediction of the ARW. For the temperature closer to T_C and the considered time the system already approaches equilibrium and we see a behavior describable by the Ornstein-Zernicke function also included in the figure.

To complete our proof that the ARW is the correct description of the ordering kinetics in the quasi-one-dimensional Ising model we will finally use a prediction of the ARW for the case where one starts with a finite initial magnetization $m(0) \neq 0$. We prepare one system with $M = 2800$, $L = 7$, $T = 0.5T_C$ and an initial probability of plus spins of $p_{\text{initial}} = 0.5$ (system I) and another with $p_{\text{initial}} = 0.6$ (system II). According to the ARW, the ratio of the diffusion coefficients for the domain walls in the two systems should be equal to

$$\frac{d_I}{d_{II}} = (1 - \tilde{m}^2) \quad (42)$$

where \tilde{m} is the magnetization at the beginning of the one-dimensional behavior. Note that we will have a two-dimensional ordering at the beginning where the magnetization changes from the initial one. We measure a ratio $d_I/d_{II} = 0.25$, which means $\tilde{m} = 1/\sqrt{2}$. Figure 13 shows the initial time

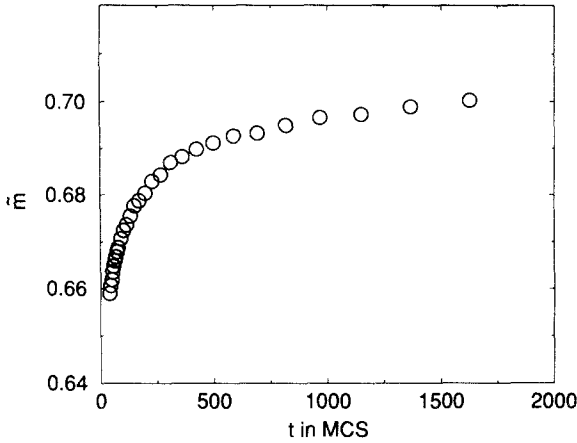


Fig. 13. Ratio of the mean overall magnetization to that inside a domain denoted as \tilde{m} , and its approach to the predicted saturation value of $1/\sqrt{z} \approx 0.707$.

dependence of \tilde{m} and its saturation at the value predicted by the ARW. During the one-dimensional ordering the mean magnetization in the system should then be constant and the mean squared magnetization should grow like (we take the mean magnetization inside a domain to be $m_T = 1$)⁽²⁸⁾

$$\langle m^2(t) \rangle = \tilde{m}^2 + \frac{2}{M\pi} (1 - \tilde{m}^2)^2 \langle l(t) \rangle \tag{43}$$

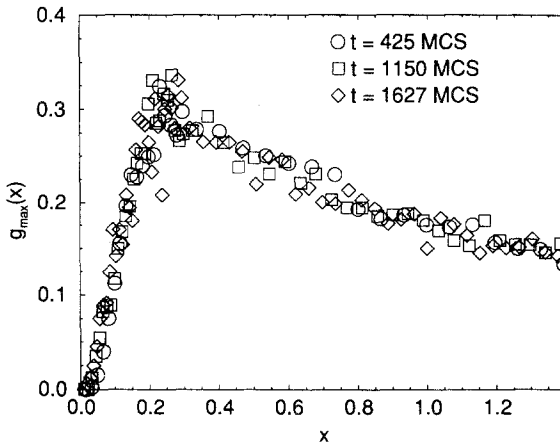


Fig. 14. Scaling plot of the domain size distribution for the majority domains. The scaling variable is $x = l/\langle l \rangle$. Times are $t = 425$ MCS (circles), $t = 1150$ MCS (squares), and $t = 1627$ MCS (diamonds).

The constancy of the mean magnetization can be understood as follows:

$$\begin{aligned} \langle m(t) \rangle &= \frac{1}{2\langle l(t) \rangle} [\langle l(t) \rangle_{\max} - \langle l(t) \rangle_{\min}] \\ &= \int dl \frac{l}{\langle l(t) \rangle} [P_{\max}(l, t) - P_{\min}(l, t)] \end{aligned} \quad (44)$$

$$= \int dx [g_{\max}(x) - g_{\min}(x)] x = \tilde{m} \quad (45)$$

where we have substituted $x = l/\langle l(t) \rangle$ and assumed independent scaling behavior for the majority as well as the minority domains:

$$\begin{aligned} P_{\max}(l, t) &= \frac{1}{\langle l(t) \rangle} g_{\max}\left(\frac{l}{\langle l(t) \rangle}\right) \\ P_{\min}(l, t) &= \frac{1}{\langle l(t) \rangle} g_{\min}\left(\frac{l}{\langle l(t) \rangle}\right) \end{aligned} \quad (46)$$

This means that the mean size of the majority domains as well as that of the minority domains grow in time, leaving the mean magnetization constant. Figures 14 and 15 show this scaling behavior for the system II and the majority and minority domains, respectively. Figure 16, finally, is a comparison of the distribution functions of the majority and minority

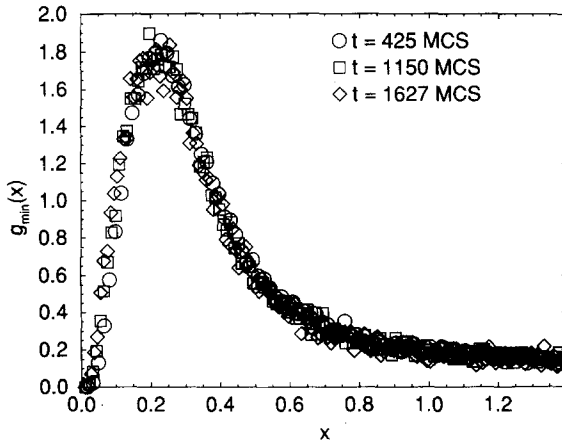


Fig. 15. Scaling plot of the domain size distribution for the minority domains. The scaling variable is $x = l/\langle l \rangle$. Times are $t = 425$ MCS (circles), $t = 1150$ MCS (squares), and $t = 1627$ MCS (diamonds).

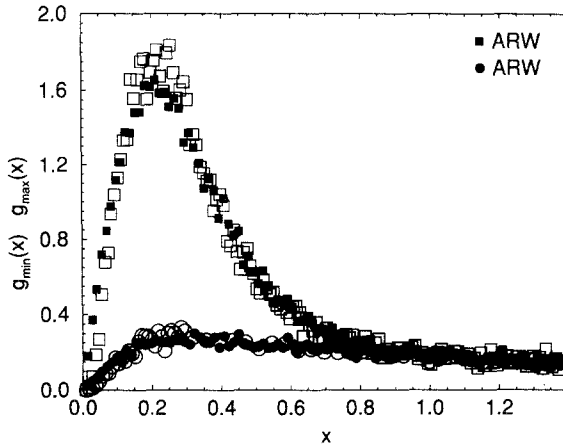


Fig. 16. Comparison of the scaling functions for the majority and minority domains in the Ising model and in the ARW. The data for the Ising model are those for $t = 1627$ MCS from Figs. 14 and 15 (minority: open squares; majority: open circles). Those for the ARW are for a simulation time of 100 walker-steps (minority: full squares; majority: full circles), which has a comparable mean domain size.

domains in the Ising model and in the ARW. The choice of times used in the comparison is again given by the requirement that the mean domain size in the two models should be equal for those times.

7. CONCLUSIONS

We have studied the ordering kinetics in an Ising strip with free boundaries in the short direction and periodic boundaries in the long direction. The kinetics show a crossover from two-dimensional to one-dimensional behavior. We have defined several quantities that measure the length scale over which the ordering has proceeded and which are applicable in the two-dimensional regime and quasi-one-dimensional regime ($\langle m^2 \rangle$ and $1/\Delta q_{||}$) or in the quasi-one-dimensional regime only (l_1 and l_2). All the length scales show the ordering process to be purely diffusive in nature, and starting at times where one can identify domain walls running across the terrace, one can describe the complete spatiotemporal behavior of the ordering process in terms of an annihilating random walk of domain walls. The possibility of a logarithmic growth law for the mean domain size in the crossover region between two-dimensional and one-dimensional growth can be ruled out. This is in contrast to the picture of Kawasaki and co-workers describing the ordering as the dynamics of kinks and anti-kinks interacting with an exponentially decreasing strength when one neglects the

stochastic forces. Our discussion of the mean-field-like approximation of the kinetics showed that this can be due to a principal difference between a discrete system with strictly finite interaction range and a continuum approximation where an interaction of infinite range is produced.

ACKNOWLEDGMENTS

It is a great pleasure to thank K. Binder for many helpful discussions. Partial support by the SFB262 is also gratefully acknowledged.

REFERENCES

1. J. D. Gunton, M. San Miguel, and P. S. Sahni, in *Phase Transitions and Critical Phenomena*, Vol. VIII, C. Domb and J. L. Lebowitz, eds. (Academic Press, New York, 1983), p. 267.
2. H. Furukawa, *Adv. Phys.* **34**:703 (1985).
3. K. Binder and D. W. Heermann, in *Scaling Phenomena in Disordered Systems*, R. Pynn and D. Skjeltorp, eds. (Plenum Press, New York, 1985), p. 207.
4. O. G. Mouritsen, in *Kinetics of Ordering and Growth at Surfaces*, M. G. Lagally, ed. (Plenum Press, New York, 1990), p. 1.
5. K. Binder, in *Kinetics of Ordering and Growth at Surfaces*, M. G. Lagally, ed. (Plenum Press, New York, 1990), p. 131.
6. K. Binder, in *Phase Transformations in Materials*, P. Haasen, ed., Weinheim, 1991), p. 405.
7. G. C. Wang and T. M. Lu, *Phys. Rev. Lett.* **50**:2014 (1983).
8. P. K. Wu, J. H. Perepesko, J. T. McKinney, and M. G. Lagally, *Phys. Rev. Lett.* **51**:1577 (1983).
9. M. C. Tringides, P. K. Wu, W. Moritz, and M. G. Lagally, *Ber. Bunsenges. Phys. Chem.* **90**:277 (1986).
10. M. C. Tringides, P. K. Wu, and M. G. Lagally, *Phys. Rev. Lett.* **59**:315 (1987).
11. P. K. Wu, M. C. Tringides, and M. G. Lagally, *Phys. Rev. B* **39**:7595 (1989).
12. M. Henzler and H. Busch, *Phys. Rev. B* **41**:4891 (1990).
13. E. V. Albano, K. Binder, D. W. Heermann, and W. Paul, *Z. Phys. B* **77**:445 (1989).
14. E. V. Albano, K. Binder, D. W. Heermann, and W. Paul, *Surf. Sci.* **223**:151 (1989).
15. E. V. Albano, K. Binder, D. W. Heermann, and W. Paul, *J. Chem. Phys.* **91**:4700 (1989).
16. E. V. Albano, K. Binder, D. W. Heermann, and W. Paul, *J. Stat. Phys.* **61**:161 (1990).
17. K. Kawasaki and T. Nagai, *Physica A* **121**:175 (1983).
18. T. Nagai and K. Kawasaki, *Physica A* **120**:587 (1983); **134**:483 (1986).
19. K. Kawasaki and T. Nagai, *J. Phys. C* **19**:L551 (1986).
20. K. Kawasaki, A. Ogawa, and T. Nagai, *Physica B* **149**:97 (1988).
21. P. Erdős and P. Ney, *Ann. Prob.* **2**:828 (1974).
22. M. Bramson and D. Griffeath, *Ann. Prob.* **8**:183 (1980).
23. D. Balding and P. Clifford, *Phys. Lett. A* **126**:481 (1988).
24. A. A. Lushnikov, *Sov. Phys. JETP* **64**:811 (1986).
25. A. A. Lushnikov, *Phys. Lett. A* **120**:135 (1987).
26. J. L. Spouge, *Phys. Rev. Lett.* **60**:871 (1988).
27. J. G. Amar and F. Family, *Phys. Rev. A* **41**:3258 (1990).

28. F. Family and J. G. Amar, *J. Stat. Phys.* **65**:1235 (1991).
29. V. Privman, *J. Stat. Phys.* **69**:629 (1992).
30. M. E. Fisher, *J. Phys. Soc. Jpn. Suppl.* **26**:87 (1969).
31. M. E. Fisher and V. Privman, *J. Stat. Phys.* **33**:385 (1983).
32. E. V. Albano, K. Binder, D. W. Heermann, and W. Paul, *Physica A* **183**:130 (1992).
33. I. M. Lifshitz, *Sov. Phys. JETP* **15**:939 (1962).
34. A. Milchev, K. Binder, and D. W. Heermann, *Z. Phys. B* **63**:521 (1986).
35. M. Müller, Diplomarbeit, Universität Mainz, unpublished.
36. M. Müller and W. Paul, in preparation.